IEEE Access
Multidisciplinary : Rapid Review : Open Access Journal

Received 24 July 2025, accepted 12 August 2025, date of publication 22 August 2025, date of current version 8 September 2025.

Digital Object Identifier 10.1109/ACCESS.2025.3602003

APPLIED RESEARCH

Use of Impedance for Condition Assessment of HV Silicone-Coated Insulators

RODRIGO J. VILLALOBOS[1], EDUARDO RICHARD[1], LUIS A. MORAN[2], (Life Fellow, IEEE), AND G. CRISTIAN PESCE[1], (Member, IEEE)

[1]Department of Electrical Engineering, Universidad de La Frontera, Temuco 4811230, Chile
[2]Department of Electrical Engineering, Universidad de Concepción, Concepción 4030000, Chile

Corresponding author: Rodrigo J. Villalobos (rodrigo.villalobos@ufrontera.cl)

This work was supported in part by ANID Startup Ciencia under Grant SUC240243, and in part by the Fondap SERC under Grant 15110019.

ABSTRACT Flashover due to contamination of glass insulators is common in electrical systems. An alternative to prevent such failures is the use of silicone-coated glass insulators. Silicone is hydrophobic, which prevents humidity from being deposited on the surface; therefore, the adhesion of environmental contaminants on the insulator is reduced. This prevents breakdowns and enables less frequent maintenance. However, in certain areas, silicone can lose its hydrophobic property, which causes contaminants to accumulate on the insulator surface. Consequently, evaluating the condition of silicone-coated insulators is essential to ascertaining their need for replacement. This requires a method that distinguishes between contamination and aging of the insulators. This paper presents the design of a machine learning classifier using a support vector machine (SVM) model that uses leakage current parameters to classify the condition of the silicone. As a distinguishing feature, the SVM classifier employs the root mean square (RMS) impedance magnitude and harmonic impedances as input parameters. This achieves an accuracy of 99% compared to 65% with data that lacked impedance measurements. The tests were conducted with insulators removed from a 500 kV line and evaluated within an artificial fog chamber.

INDEX TERMS Insulators, silicone rubber, machine learning, leakage current, aged, pollution level estimation.

I. INTRODUCTION

Single-phase ground-fault insulator strings are common in substations [1]. These faults also occur in overhead lines [2] and transmission lines [3]. These failures are largely caused by contaminants adhering to the insulator surface. The contamination is contingent upon the geographic location and the surrounding environment of the insulator string. Ground faults known as flashovers [4] occur due to the interaction of contaminants [5] with ambient humidity [6]. This increases the leakage current amplitude of the insulator [4]. These costs are associated with the need for specialists [7] and the large volumes of water required [8]. To prevent flashovers, electrical companies perform maintenance at irregular intervals (e.g., 1, 3, 6, and 12 months). Insulator maintenance is conducted by washing with pressurized demineralized water [9]. Although this solution mitigates the occurrence of faults, it incurs high costs for companies. One alternative to increase the interval between washing is to use composite silicone rubber insulators (SiRs). Another alternative is silicone-coated glass insulators. Silicone has a high humidity repellency due to its hydrophobic characteristics. This property reduces the adhesion of contaminants to the insulator surface. Hydrophobicity also helps prevent the formation of a contaminated water layer, thus avoiding flashovers. However, silicone rubber materials have been reported to lose their hydrophobic properties over time [10], [11]. This can be caused by solar UV radiation [12], [13], [14] and the corona effect [15]. The above conditions degrade the silicone, allowing environmental contaminants to adhere to the surface, similar to what occurs in glass insulators. Therefore, companies must periodically inspect

The associate editor coordinating the review of this manuscript and approving it for publication was Ahmed A. Zaki Diab.

their silicone-coated insulators to assess their condition. Inspection helps determine whether they are aging with loss of hydrophobicity or are contaminated. Some studies have attempted to enhance the hydrophobic properties of SiR insulators [16], [17]. These studies evaluated different compounds to improve the hydrophobicity of the materials and counteract exposure time effects. However, these nanocomposite-based solutions are expensive for large-scale production and have not yet been widely implemented [18]. The literature reports advances in determining the conditions of both glass and silicone-coated insulators, focusing mainly on leakage current analysis. In [19], the authors endeavored to recreate the shape and amplitude of leakage current in fully and partially silicone-coated insulators. They used the random forest algorithm with the Cumulative Pollution Index (CPI) for prediction. The algorithm achieves a high average coefficient of determination (R^2) of 86% for contamination. However, the paper does not address material aging. The paper [20] employs a supervised support vector machine (SVM) learning algorithm to classify erosion and contamination in silicone-coated glass insulators. The authors reported a 100% accuracy. However, erosion is simulated in a laboratory environment by mechanically scratching the silicone. This type of degradation has not been reported in other studies and may not accurately represent natural aging over time. In [21], the authors applied the Stockwell transform and various other classifiers. The success of the random forest algorithm, with an accuracy of 97.14%, was highlighted. However, these approaches fail to address the impact of aging on polymeric materials. In [22] the researchers used neural networks to predict leakage currents in highly aged polymeric insulators. That paper described promising results but focused on differentiating the effects of contamination and aging separately in these insulators. Various studies have demonstrated that the leakage current can accurately identify contamination levels in silicone-coated insulators. Additionally, other studies have identified aging levels in these insulators. However, no single tool has been developed to discriminate between aging and contamination. As mentioned, this differentiation is crucial for electric companies as procedures vary depending on whether the insulators are contaminated or aged. In [23] reported on the relationship between the impedance of a glass insulator and environmental conditions, such as contamination deposited on the surface of the insulator and the humidity to which they are exposed. The authors found that the impedance of the glass insulator decreased with increasing humidity and contamination.

This study proposes to use RMS impedance and harmonic impedances as diagnostic parameters to distinguish between aging and contamination in silicon-coated insulators. The impedance provides information about the physical state of the insulator. This allows for more accurate classification using the SVM algorithm. The incorporation of impedance parameters significantly improves the classification accuracy compared to methods that do not use them. To validate this approach, tests were performed in an artificial fog chamber following IEC 60507 standards. New and field-aged (three years) silicone-coated insulators from a 500 kV transmission line were analyzed in the study. The results support the development of a diagnostic tool for laboratory evaluations. This tool allows companies to more effectively evaluate insulators removed from the field. As a result, maintenance strategies can be optimized to ensure better performance and reliability.

(a) (b) (c)

FIGURE 1. Sample insulators. (a) Clean and new insulator. (b) Clean insulator with three years of service. (c) Dirty insulator with three years of service.

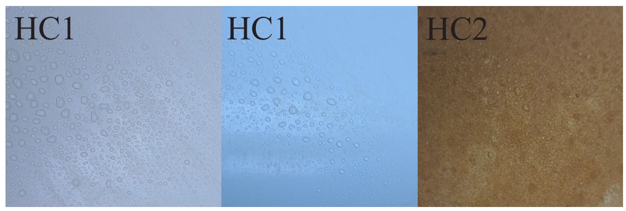

(a) (b) (c)

FIGURE 2. Hydrophobicity classes. (a) HC1. (b) HC1. (c) HC2.

II. SAMPLES EXPERIMENTAL SETUP AND PROCEDURE

This section describes the procedure and tests conducted on silicone-coated insulators at various contamination levels and humidity.

A. SAMPLES

A silicone-coated insulator was selected for the tests in three different conditions. The insulator used in the tests was model U120KN, manufactured by Sediver, with a creepage distance of 450 mm and a weight of 5.5 kg, as shown in Table 1. The differences lie in the level of contamination and years of use (aging). Fig. I(a) shows the first specimen, which is a new and uncontaminated SiR insulator. Fig. I(b) shows the second specimen, an insulator removed from a 500 kV line with 3 years of service and cleaned in the laboratory. Fig. I(c) shows the third specimen, an insulator exhibiting identical

TABLE 1. Specifications of the Silicone-coated insulator used in the tests.

Model	U120KN
Creepage distance	450 mm
Weight	5.5 kg

TABLE 2. Hydrophobicity.

	Class		
Sample	#1	#2	#3
Years of service	0	3	3
Hydrophobicity	HC1	HC1	HC2

characteristics to the removed insulator while retaining its surface contamination for testing purposes.

To classify the hydrophobicity levels of these insulators, the IEC 62073-2016 standard was used. This standard evaluates hydrophobicity by measuring the response of surface insulators briefly exposed to water. The standard classifies hydrophobicity from HC1 to HC6. HC1 had the highest hydrophobicity and HC6 the lowest. Fig. 2 shows the hydrophobicity test results for the 3 selected insulators. Table 2 lists the resulting hydrophobicity classes. Notably, the new insulator and the old insulator that was cleaned both present an HC1 class. Contaminated insulators have an HC2 class.

B. SET-UP

The three different insulators were tested inside an artificial fog chamber. The chamber fog was designed according to IEC 60507 to simulate the relative humidity conditions inside the insulators. The chamber is shown in Fig. 3(a). Fig. 3(b) shows the laboratory setup, which consisted of a $0.38/13.2\ kV$ transformer controlled by a $380V$ single-phase variac. Each insulator was suspended vertically inside the artificial fog chamber and subjected to a voltage of 9 kV. The leakage current flowing through the insulator and the voltage across the pin-cap terminals were measured during each test. The leakage current in each test is measured using a 10 $[K\Omega]$ shunt resistor connected in series with each insulator. While the voltage is measured using a Pintek DP40K voltage probe. The temperature and humidity inside the chamber were also recorded with the SHT31 sensor. Table 3 lists the tests performed. The tests were grouped according to age and contamination status. Each insulator was subjected to four tests with constant humidity levels of 60%, 80%, 90%, and 100%, respectively. Two additional tests were performed with humidity levels between 60% and 100%, respectively.

C. MEASURED ELECTRICAL CHARACTERISTICS

The leakage current and voltage were measured for each test at a sampling frequency of 25 kHz. To maintain constant humidity levels during each test, humidity sensors were installed inside the chamber to provide feedback to the control circuit to ensure the desired conditions. Subsequently, the

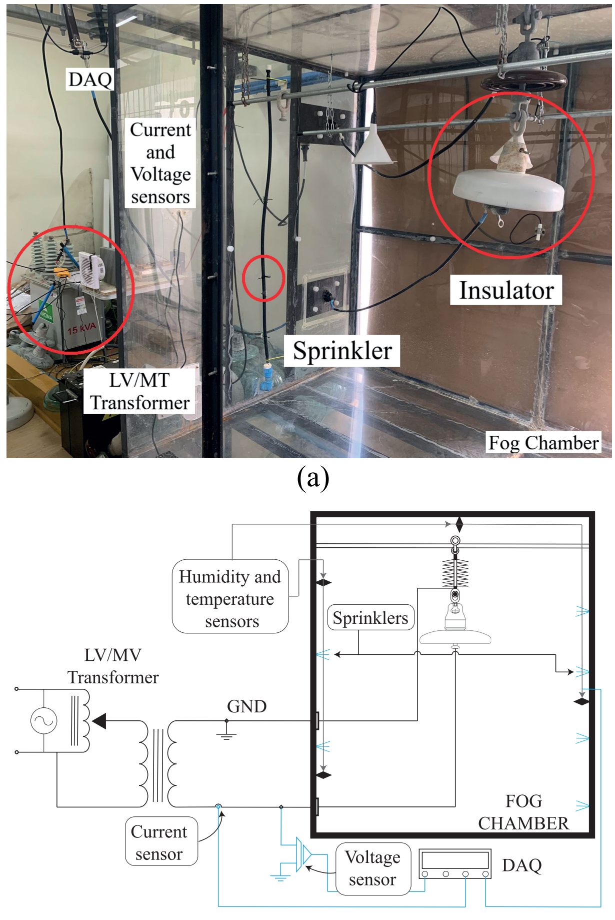

FIGURE 3. Laboratory set-up. (a) Real photography (b) Schematic design.

TABLE 3. Test in fog chamber for insulators.

		Characteristic Test			
N°Test	Aged	Hum.	State	Hum.[%]	Temp.[$^{\circ}C$]
		Normality Test			
1	New	Controlled	Clean	60	20
2	New	Controlled	Clean	80	20
3	New	Controlled	Clean	90	20
4	New	Controlled	Clean	100	20
5	3 years	Controlled	Clean	60	20
6	3 years	Controlled	Clean	80	20
7	3 years	Controlled	Clean	90	20
8	3 years	Controlled	Clean	100	20
9	3 years	Controlled	Contaminated	60	20
10	3 years	Controlled	Contaminated	80	20
11	3 years	Controlled	Contaminated	90	20
12	3 years	Controlled	Contaminated	100	20
		Additional Test			
13	3 years	Step	Clean	60 to 100	$14-16$
14	3 years	Step	Contaminated	60 to 100	$18-22$

various characteristics of the leakage current were extracted using MATLAB software. The RMS value, peak value, and 3rd, 5th, 7th, 9th, and 11th-order harmonics are included. Additionally, five indices were calculated as presented in the literature. The calculated indices include the total harmonic distortion (THD) of current and voltage [24], the ratio of the 3rd to 5th harmonic [25], the Rhi index [26], the phase shift

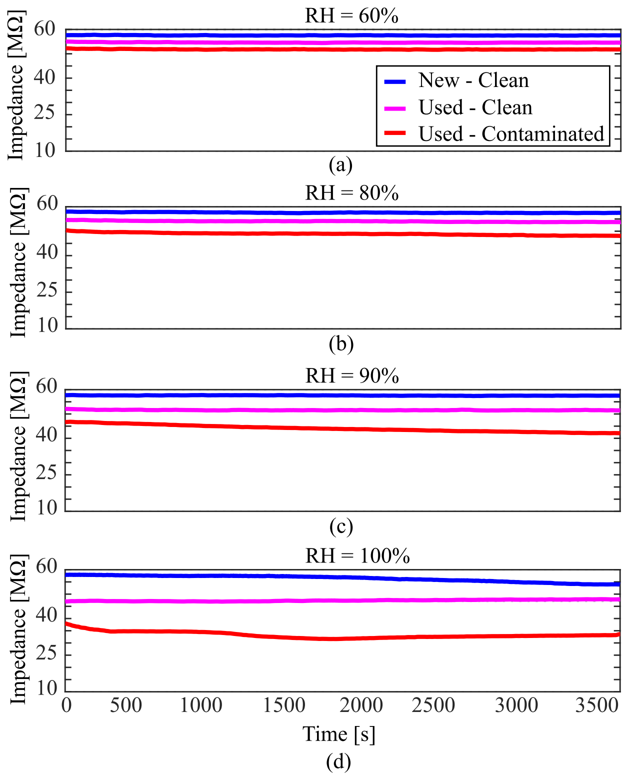

FIGURE 4. Impedance for tests separated by humidity. (a) Impedance for tests with RH = 60%. (b) Impedance for tests with RH = 80%. (c) Impedance for tests with RH = 90%. (d) Impedance for tests with RH = 100%.

of the leakage current relative to the voltage (PI) [25], and the impedance magnitude calculation (RMS and odd harmonics) of the insulator [23].

III. IMPEDANCE OF SILICONE-COATED INSULATORS

The impedance magnitude is defined as the ratio of the voltage magnitude to the leakage current magnitude. Fig. 4 shows the RMS impedance magnitude of the insulator for humidity conditions of (60%, 80%, 90%, and 100%). The blue curve represents the new-clean insulator. The magenta curve indicates the used-clean insulator. The red curve represents the used-contaminated insulator.

Notably, the impedance of the new-clean insulator presents a constant impedance value (57 MΩ) regardless of the humidity level. This may be related to the highest hydrophobicity class (HC1). Therefore, for new and clean insulators it can be said that humidity does not affect the impedance magnitude of the insulator. In the case of the used-clean insulator, the impedance decreases (51 MΩ to 47 MΩ) as the humidity increases ((60%) to (100%)). This implies that the years of use of the insulator affect the impedance. The magnitude of the impedance of the used-clean insulator decreases with increasing humidity. In the used-contaminated condition, the impedance values at (60%) humidity show a magnitude of 42 MΩ, which is lower than the previous case (51 MΩ). The values decrease to 33 MΩ when the humidity reaches (100%). In Fig. 4(d), variations in the amplitude of the RMS impedance can be observed among different silicone-coated insulators. These fluctuations are caused by the absorption and evaporation of humidity on the insulators surface. This process leads to changes in the impedance RMS.

Finally, it can be stated that the impedance of silicone-coated insulators decreases directly with aging and surface contamination. These results suggest that impedance can serve as a useful indicator for distinguishing between aging and contamination in silicone-coated insulators. The next section develops an SVM algorithm to identify the condition of insulators in terms of aging and surface contamination. The relevance of impedance as a distinctive parameter for the condition assessment of silicon-coated insulators was highlighted.

IV. MULTICLASS SVM

A supervised machine learning classification algorithm called support vector machines (SVM) was applied [27]. SVM is considered one of the most commonly used techniques for classification, prediction, and outlier detection [28]. An SVM facilitates binary classification and can be extended for multiclass classification. Thus, in this study, the insulator conditions (new-clean, used-clean, and used-contaminated) were classified using a multiclass SVM. Each models optimal hyperparameters (kernel, regularization constant C, and Γ) were determined using cross-validation in Python. The proposed SVM classification process is show in Fig. 5. The classification steps of the insulators include (i) leakage current measurement, (ii) data processing, (iii) data grouping, and (iv) application of the SVM and output results.

A. MODELS

For SVM training, 70% of the data from each test were assigned to training, and the remaining 30% were used for validation. Linear and radial basis function (RBF) kernels were used during the hyperparameter search in Python. To evaluate and compare the performance of the models, accuracy was calculated using the formula: $accuracy = [(TP + TN)/(TP + FN + TN + FP)] \cdot 100$, where TP (True Positive), TN (True Negative), FN (False Negative), and FP (False Positive) represent the classification outcomes.

1) K-FOLD CROSS VALIDATION

Cross-validation was employed to assess the generalization capability of classification models across various datasets [24]. This technique avoids over-adjustment and ensures reliable performance. For example, in [29], cross-validation is applied to train and validate a classification model for insulator hydrophobicity using surface images. The images were divided into five partitions ($k = 5$). In [30], an algorithm was proposed to classify contamination in ceramic insulators. They used cross-validation to train the model and optimize the hyperparameters. Python libraries suggest optimal partitions of $k = 5$ and $k = 10$. A cross-validation algorithm with $k = 5$ was implemented

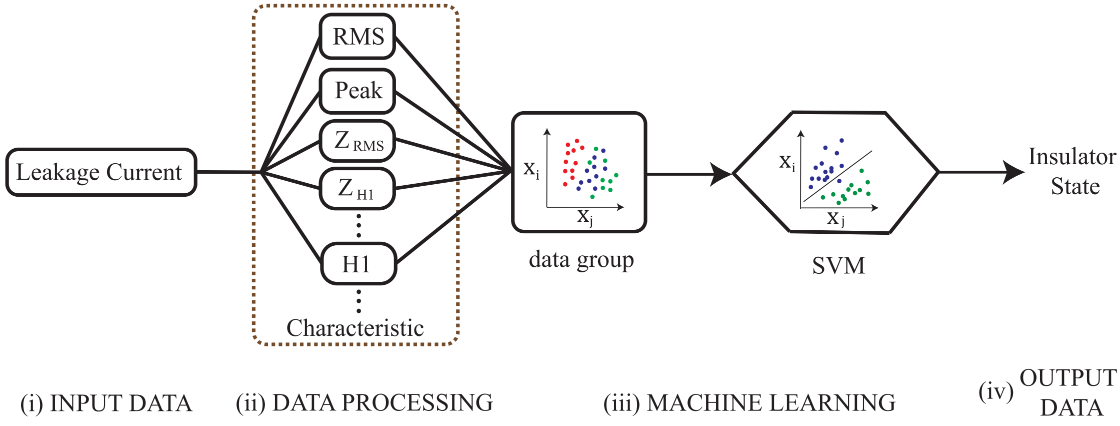

FIGURE 5. General scheme of the proposed SVM-based classification model.

to tune and optimize the hyperparameters of the designed models.

B. TRAINING AND VALIDATION OF CLASSIFICATION MODELS

A dataset of 820,800 data points, obtained from 12 laboratory tests, was used to train ten SVM classification models. These models were developed to assess the aging and contamination state of silicone-coated insulators. The first four models use leakage current features. These include the RMS value, peak value, total harmonic distortion, harmonics, and harmonic-derived indices. Additionally, these models consider the total RMS impedance of the insulator and the harmonic impedances of the 3rd, 5th, 7th, 9th, and 11th orders. For the six models that do not use impedance data, a subset of 518,400 data points from the original dataset was used. This subset does not include RMS impedance values or harmonic impedance data. Two of these six models without impedance were configured as SVM cascades. The first cascade model classifies aging, while the second classifies contamination.

Fig. 6 shows the development of these 10 models. The twelve initial tests listed in Table 3 were used to generate the models. 70% of the data from each test were used for training the models, and the remaining 30% were used for validation. The 70% leakage current parameters were calculated and divided into two groups: with and without impedance.

The training data generated eight subsets labeled G1, G2, G3, G4, G5, G6, G7, and G8. Subsets G1 and G5 were used to create Model 1 for data with impedance and Model 1 for data without impedance, respectively. These models were trained using tests 1, 2, 4, 5, 6, 8, 9, 10, and 12. For validation, 30% of the remaining data from these tests, along tests 3, 7, and 11, were used for G1 and G5, respectively. Similarly, subsets G2 and G6 were used to create Model 2 for data with impedance and Model 2 for data without impedance, respectively. These models were trained using tests 1, 3, 4, 6, 8, 9, 10, and 12. For validation, 30% of the remaining data from these tests, along tests 2, 5, 7, and 11, were used for G2 and G6, respectively. Subsets G3 and G7 were used to create Model 3 for data with impedance and Model 3 for data without impedance, respectively. These models were trained using tests 2, 5, 7, and 11. For validation, tests 1, 3, 4, 6, 8, 9, 10, and 12, along 30% of the training tests, were used for G3 and G7, respectively. Subset G4 and G8 was used to create Model 4 for data with impedance and Model 4 for data without impedance, respectively. A random selection of 500 data points per parameter from each test (1 to 12) was used for training. The selected data points for the model with impedance were different from those used for the model without impedance. For validation, an additional 500 random data points per parameter from each test (1 to 12), distinct from those used in training, were selected. The validation data for the model with impedance were also different from those used for the model without impedance. Cross-validation was applied to each model using the training subsets to optimize hyperparameters and prevent overfitting.

Cascade Models 1 and 2 were trained with subsets G7 and G8, respectively, along with their corresponding validation subsets. Using the training and validation subsets, along with cross-validation, a Python code was implemented that provides the accuracy parameter of the SVM models.

Finally, Fig. 6 shows the accuracy of the 10 models with validation data. It was noted that models incorporating impedance information achieved accuracies between 80% and 100%, with an average of 95%. This was achieved without increasing the complexity and computational load of the classifier training. Models that did not consider impedance yielded an accuracy between 31% and 100%, averaging 53%. However, the cascade model configuration improved the accuracy by approximately 30%. Results obtained with impedance values presented a substantial advantage, showing an accuracy of over 80% for identifying aging and contamination in silicone-coated insulators.

Moreover, Model 4 stands out for its high capability to evaluate insulator conditions with 100% accuracy for cases with and without impedance data. Its high performance

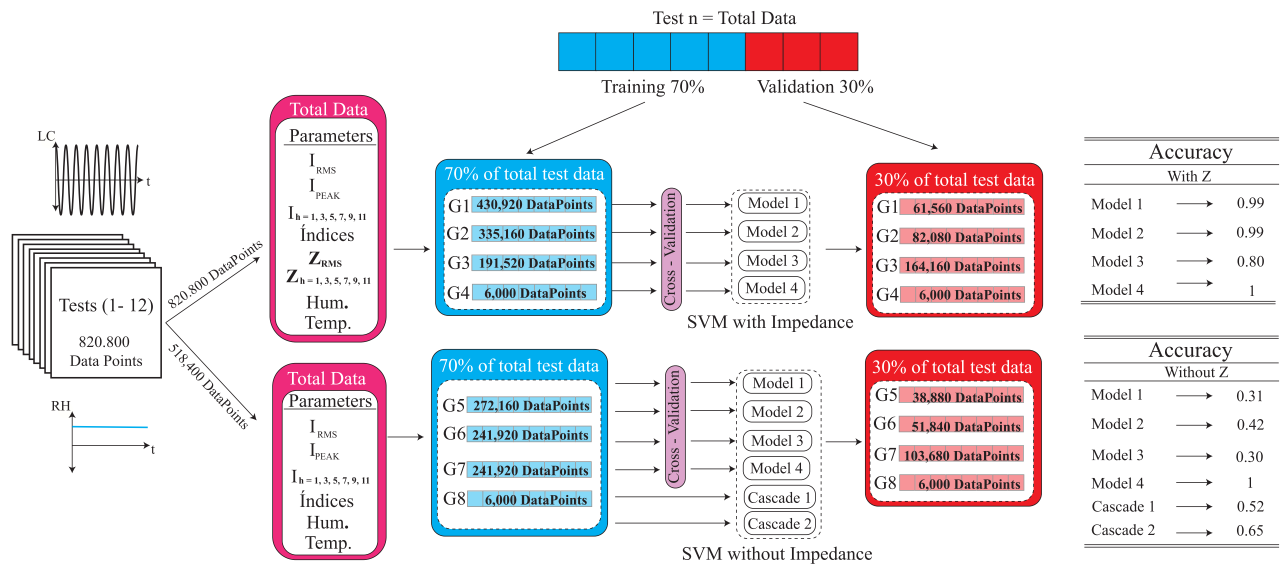

FIGURE 6. Construction of SVM models with and without impedance.

is related to the small amount of data used for training and validation, resulting in minimal variability between the training and validation stages.

To assess the robustness of the classification models with data and tests different from those used in training and validation, the SVM models were tested with new tests and humidity scenarios. This is discussed in the following section.

V. ROBUSTNESS OF THE CLASSIFICATION ALGORITHM

This section evaluates the 10 developed models using tests that are different from those in the validation stage. In contrast to the tests used in the training and validation stage, Tests 13 and 14 simulate conditions of humidity that are not constant. Tests 13 and 14 simulate a humidity ramp from 60% to 100% over 30 minutes for both the new-clean insulator and the used-contaminated insulator.

Table 4 summarizes the accuracy results for all the developed models. Notably, for Tests 13 and 14, Models 1, 2, 3 and 4 exhibited higher accuracy with impedance parameters than the models without impedance. On average, incorporating impedance increases the accuracy by 32%. In test 13, Model 4 produced a 35% increase in accuracy when using RMS impedance and harmonics as input parameters. Models with impedance achieved a maximum accuracy of 99%. Conversely, implementing cascade SVM models without impedance enhances classification accuracy for Tests 13 and 14 by up to 52% and 62%, respectively.

Model 4 for Test 14 was selected for graphical representation since its results exhibit variation in Table 4. Fig. 7 graphically illustrates the accuracy of the developed models. Three states for classification were defined: State 1 for new-clean insulators, State 2 for used-clean insulators, and State 3 for used-contaminated insulators. The dashed black line

TABLE 4. Comparison of the accuracy parameter for the results obtained for each SVM classification model.

	Accuracy	
Model	Without Z	With Z
Test N°13		
1	0	0.39
2	0	0.40
3	0.02	0.29
4	0	0.96
Cascade 1	0.25	–
Cascade 2	0.52	–
Test N°14		
1	0.54	0.99
2	0.49	0.99
3	0.99	0.99
4	0.58	0.23
Cascade 1	0.51	–
Cascade 2	0.62	–

represents the actual state of the insulator during the test. Models trained with impedance data are shown with a green background, whereas models without impedance data are shown with a yellow background. The red dots indicate the classification result of the insulator state provided by the SVM.

Fig. 7(a) shows the accuracy of Model 4 for Test 13. It is observed that the model incorporating impedance shows a significantly higher accuracy than the model without impedance. The impedance-based classification achieved an accuracy of 96%, whereas the non-impedance model achieved an accuracy of 0%. Fig. 7(b) shows the accuracy of Model 4 in Test 14. The impedance-based classification achieved an accuracy of 23%, whereas the non-impedance model achieved an accuracy of 58%. In this particulare case, the non-impedance model demonstrated higher accuracy.

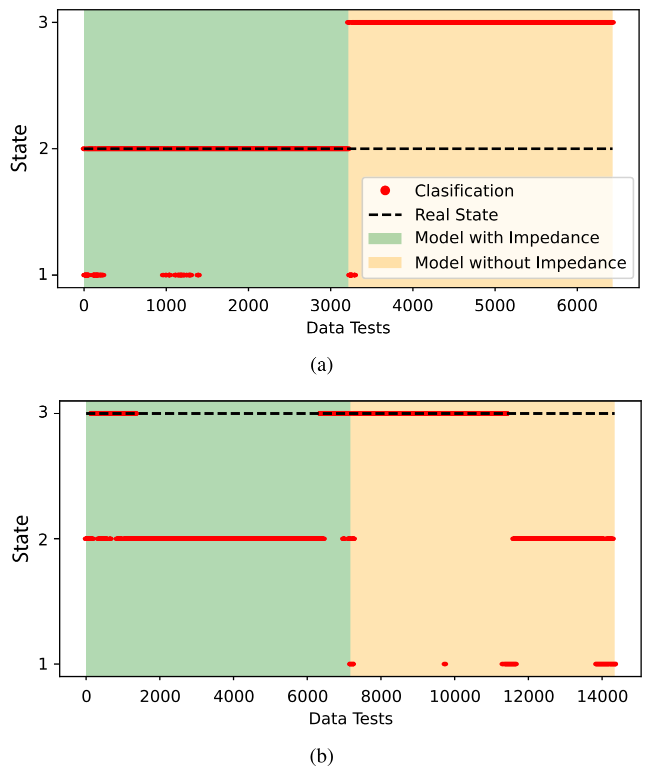

FIGURE 7. **Classification results for model 4 SVM. (a) Model 4 - Test 13. (b) Model 4 - Test 14.**

This was due to the high RMS currents recorded during Test 14 due to the sudden increase in chamber humidity (ramping tests). Specifically, the RMS current magnitudes exceeded 0.3 mA in this test, whereas in other tests, the magnitudes did not exceed 0.28 mA. To ensure model validity, tests with constant humidity were used to maintain the training conditions of the SVM model.

Model 4 showed preliminary limitations at higher current levels. This is because Model 4 was trained on a small data set (500 points), randomly selected per test, which was insufficient to cover the full range of current levels for Test 14. On the other hand, the models were trained on data from constant humidity levels instead of tests 13 and 14, which showed a rapid increase in humidity from 60% to 100%, causing a sudden increase in leakage current. To ensure reliable performance, it is imperative that the newly implemented laboratory tests match the controlled humidity conditions used during model training.

VI. CONCLUSION

This study proposes a method to classify the condition of silicone-coated insulators using a Support Vector Machine (SVM) approach incorporating insulator impedance data. The relevance of including both RMS impedance and harmonic impedances in the training process of SVM models for silicone-coated insulators was demonstrated. The SVM model without impedance data achieved a maximum accuracy of 65%, while the model incorporating impedance data reached 99% during training. Furthermore, the SVM model with impedance maintained an average minimum accuracy of 80%, compared to only 31% for the model without impedance. The proposed SVM approach effectively distinguishes between new-clean, used-clean, and used-contaminated states of silicone-coated insulators, achieving a maximum accuracy of 99% in tests. It has been demonstrated that the SVM models developed for the identification of states in insulators exhibit sensitivity to humidity conditions and the quantity of data utilized during the training stage. To illustrate this, tests 13 and 14 were incorporated to demonstrate that the accuracy of the models reaches 23% when Model 4 is employed, a model that utilizes a limited number of points (500 data points) and is executed under non-constant humidities.

Ultimately, the inclusion of RMS and harmonic impedance data significantly improves the accuracy of SVM models, allowing for a reliable assessment of the condition of silicone-coated insulators.

REFERENCES

[1] L. Liu, H. Mei, C. Guo, Y. Tu, and L. Wang, "Pixel-level classification of pollution severity on insulators using photothermal radiometry and multiclass semisupervised support vector machine," *IEEE Trans. Ind. Informat.*, vol. 17, no. 1, pp. 441–449, Jan. 2021.

[2] G. Liu, Y. Wen, Y. Gu, F. Guo, J. Zhou, X. Zhang, and S. Chen, "Monitoring of composite insulators in transmission lines: A hydrophobicity diagnostic method using aerial images and residual neural networks," *IEEE Trans. Power Del.*, vol. 38, no. 4, pp. 2500–2509, Aug. 2023.

[3] L. Xin, H. Jin, Y. Tu, Z. Yuan, Z. Lv, and C. Wang, "Defect detection and characterization of RTV silicone rubber coating on insulator based on visible spectrum image," *IEEE Trans. Power Del.*, vol. 35, no. 6, pp. 2734–2736, Dec. 2020.

[4] R. J. Villalobos, L. A. Moran, F. Huenupán, F. Vallejos, R. Moncada, and C. Pesce G., "A new current transducer for on-line monitoring of leakage current on HV insulator strings," *IEEE Access*, vol. 10, pp. 78818–78826, 2022.

[5] S. S. Roy, A. Paramane, J. Singh, S. Chatterjee, and A. K. Das, "Accurate sensing of insulator surface contamination using customized convolutional neural network," *IEEE Sensors Lett.*, vol. 7, no. 1, pp. 1–4, Jan. 2023.

[6] Y. Mizuno, M. Maeda, and K. Kondo, "Flashover risk-based probabilistic design of transmission line insulators under contamination conditions," *IEEE Trans. Power Del.*, vol. 38, no. 5, pp. 3611–3620, Oct. 2023.

[7] M. E. Ibrahim and A. M. Abd-Elhady, "Rogowski coil transducer-based condition monitoring of high voltage insulators," *IEEE Sensors J.*, vol. 20, no. 22, pp. 13694–13703, Nov. 2020.

[8] *Outdoor Insulation in Polluted Conditions: Guidelines for Selection and Dimensioning—Part 1: General Principles and the A.C. Case*, CIGRE, Paris, France, 2008.

[9] R. Castillo-Sierra, O. Oviedo-Trespalacios, J. E. Candelo-Becerra, J. D. Soto, and M. Calle, "A novel method for prediction of washing cycles of electrical insulators in high pollution environments," *Int. J. Electr. Power Energy Syst.*, vol. 130, Sep. 2021, Art. no. 107026.

[10] Z. Zeng, P. Guo, R. Zhang, Z. Zhao, J. Bao, Q. Wang, and Z. Xu, "Review of aging evaluation methods for silicone rubber composite insulators," *Polymers*, vol. 15, no. 5, p. 1141, Feb. 2023.

[11] K. Sit, A. K. Pradhan, B. Chatterjee, and S. Dalai, "A review on characteristics and assessment techniques of high voltage silicone rubber insulator," *IEEE Trans. Dielectr. Electr. Insul.*, vol. 29, no. 5, pp. 1889–1903, Oct. 2022.

[12] L. Cheng, Y. Liu, R. Chen, S. Zhang, R. Liao, L. Yang, and T. Wang, "Method for predicting the water absorption of external insulating silicone rubber," *IEEE Trans. Dielectr. Electr. Insul.*, vol. 29, no. 4, pp. 1242–1250, Aug. 2022.

[13] A. A. Nekahi, S. G. McMeekin, and M. Farzaneh, "Measurement of surface resistance of silicone rubber sheets under polluted and dry band conditions," *Electr. Eng.*, vol. 100, no. 3, pp. 1729–1738, Sep. 2018.
[14] D. Ghosh and D. Khastgir, "Degradation and stability of polymeric high-voltage insulators and prediction of their service life through environmental and accelerated aging processes," *ACS Omega*, vol. 3, no. 9, pp. 11317–11330, Sep. 2018.
[15] B. Thangabalan, Neelmani, N. J. Vasa, R. Sarathi, N. Harid, and H. Griffiths, "Understanding the surface condition of silicone rubber nanocomposite due to corona aging using AFM imaging and LIBS spectroscopy," *IEEE Trans. Dielectr. Electr. Insul.*, vol. 29, no. 6, pp. 2089–2100, Dec. 2022.
[16] H. de Santos and M. Á. Sanz-Bobi, "Research on the pollution performance and degradation of superhydrophobic nano-coatings for toughened glass insulators," *Electric Power Syst. Res.*, vol. 191, Feb. 2021, Art. no. 106863.
[17] Y. Liu, Y. Guo, B. Wang, X. Zhang, G. Huang, G. Zhang, Y. Liu, Q. Deng, and G. Wu, "Pollution morphology characteristics on a superhydrophobic surface and its pollution flashover voltage in DC electric field," *High Voltage*, vol. 7, no. 3, pp. 564–574, Jun. 2022.
[18] A. Allahdini, G. Momen, F. Munger, S. Brettschneider, I. Fofana, and R. Jafari, "Performance of a nanotextured superhydrophobic coating developed for high-voltage outdoor porcelain insulators," *Colloids Surf. A, Physicochemical Eng. Aspects*, vol. 649, Sep. 2022, Art. no. 129461.
[19] H. de Santos and M. A. Sanz Bobi, "A cumulative pollution index for the estimation of the leakage current on insulator strings," *IEEE Trans. Power Del.*, vol. 35, no. 5, pp. 2438–2446, Oct. 2020.
[20] A. A. Salem, K. Y. Lau, Z. Abdul-Malek, and C. W. Tan, "Classifying insulator conditions of room temperature vulcanized coated glass insulators under different coating damage modes," *Measurement*, vol. 194, May 2022, Art. no. 111032.
[21] K. Sit, A. K. Das, D. Mukherjee, N. Haque, S. Deb, A. K. Pradhan, S. Dalai, and B. Chatterjee, "Condition monitoring of overhead polymeric insulators employing hyperbolic window stockwell transform of surface leakage current signals," *IEEE Sensors J.*, vol. 21, no. 9, pp. 10957–10964, May 2021.
[22] A. A. Salem, A. A. Alawady, K. Y. Lau, W. Rahiman, Z. Abdul-Malek, S. A. Al-Gailani, S. M. Al-Ameri, E. Ali, and S. S. M. Ghoneim, "Investigating and modeling ageing effects on polymeric insulator electrical properties," *IEEE Access*, vol. 11, pp. 82132–82150, 2023.
[23] R. J. Villalobos, L. A. Moran, M. Inostroza, A. Hoffer, G. C. Pesce, and F. Huenupán, "Humidity and harmonic current considerations for indices to estimate contamination levels on HV insulators," *IEEE Access*, vol. 11, pp. 130931–130941, 2023.
[24] A. A. Salem, R. Abd-Rahman, S. A. Al-Gailani, M. S. Kamarudin, H. Ahmad, and Z. Salam, "The leakage current components as a diagnostic tool to estimate contamination level on high voltage insulators," *IEEE Access*, vol. 8, pp. 92514–92528, 2020.
[25] M. F. Palangar, S. Mohseni, A. Abu-Siada, and M. Mirzaie, "Online condition monitoring of overhead insulators using pattern recognition algorithm," *IEEE Trans. Instrum. Meas.*, vol. 71, pp. 1–11, 2022.
[26] A. A. Salem, R. Abd-Rahman, S. A. Al-Gailani, Z. Salam, M. S. Kamarudin, H. Zainuddin, and M. F. M. Yousof, "Risk assessment of polluted glass insulator using leakage current index under different operating conditions," *IEEE Access*, vol. 8, pp. 175827–175839, 2020.
[27] M. Sheykhmousa, M. Mahdianpari, H. Ghanbari, F. Mohammadimanesh, P. Ghamisi, and S. Homayouni, "Support vector machine versus random forest for remote sensing image classification: A meta-analysis and systematic review," *IEEE J. Sel. Topics Appl. Earth Observ. Remote Sens.*, vol. 13, pp. 6308–6325, 2020.
[28] J. Cervantes, F. Garcia-Lamont, L. Rodríguez-Mazahua, and A. Lopez, "A comprehensive survey on support vector machine classification: Applications, challenges and trends," *Neurocomputing*, vol. 408, pp. 189–215, Sep. 2020.
[29] S. Chatterjee, S. S. Roy, K. Samanta, and S. Modak, "Sensing wettability condition of insulation surface employing convolutional neural network," *IEEE Sensors Lett.*, vol. 4, no. 7, pp. 1–4, Jul. 2020.
[30] A. K. Das, S. Deb, D. Dey, B. Chatterjee, and S. Dalai, "Multisynchrosqueezing transform based improved time-frequency representation for automated contamination severity estimation of overhead line insulator," *IEEE Sensors J.*, vol. 22, no. 12, pp. 12098–12106, Jun. 2022.

RODRIGO J. VILLALOBOS received the Engineering degree in electrical engineering from the University of Concepción, Concepción, Chile, in 2006, the Professional Master degree in electrical engineering from Université Paris-Sud, Orsay, France, in 2008, and the Ph.D. degree from the University of Concepción, in 2024. From 2008 to 2015, he was a Project Manager for the power transmission industry in Chile, developing projects of power substations and transmission lines. Since 2015, he has been with the Electrical Engineering Department, University de La Frontera, Temuco. Since 2021, he has been a lead consultant to determine the contamination level of the new 600 kV Kimal-LoAguirre HVDC line. His research interests include power transmission systems, insulation in power systems, and practical solutions equipment for the challenge of power transmission systems industry.

EDUARDO RICHARD received the Engineering degree in electronic engineering from the University de La Frontera, Temuco, Chile, in 2020, and the M.Sc. degree in electronic engineering from Universidad Tecnica Federico Santa María (UTFSM), Valparaíso, Chile, in 2023. He is currently pursuing the Ph.D. degree with the University de La Frontera. He has worked on determining the contamination of insulators due to current leakage through a FONDEF Project. His current research interests include power transmission systems, control strategy, dc-dc converter, and machine learning.

LUIS A. MORAN (Life Fellow, IEEE) was born in Concepción, Chile. He received the degree in electrical engineering from the University of Concepción, Concepción, in 1982, and the Ph.D. degree from Concordia University, Montreal, QC, Canada, in 1990. Since 1990, he has been with the Electrical Engineering Department, University of Concepción, where he is a Professor. He has written and published more than 60 transaction papers in the design of static converters for power system dynamic compensation (var compensators and active power filters), and power quality issues in industrial power distribution systems. He has more than 30 years of full-time teaching and research activities, including short courses for industry and utility companies, and concurrent experience as industrial consultant. He has extensive consulting experience in mining industry.

G. CRISTIAN PESCE (Member, IEEE) received the degree in electronic engineering from the Pontificia Universidad Catolica de Valparaíso, Valparaíso, Chile, in 2003, the M.Sc. degree in electrical engineering from the University de La Frontera, Temuco, Chile, in 2010, and the D.Sc. degree in electrical engineering from the University of Concepción, Concepción, Chile, in 2017. He is currently an Assistant Professor with the Department of Electrical Engineering, University de La Frontera. His research interests include design and control of power converters applied to electric power systems and electrical machines and drives.